Volume 10, Issue 6
December 2021

ITEE Journal
Information Technology & Electrical Engineering

ISSN: - 2306-708X

Modulation Strategy to Eliminate Dominant Current Harmonics in Six-Phase Asymmetrical Induction Motor Drive

[1]Shaikh Mo. Suhel A and [2]Vamja Rajan Vinodray

[1]R.N.G.P.Institute of Technology, Surat-395001, India

[2]Sardar Vallabhbhai National Institute of Technology, Surat-395007, India

E-mail: [1]suhelshaikh21@gmail.com, [2]rajan.pe.svnit@gmail.com

ABSTRACT

This paper presents the development of the Space Vector PWM algorithm for dual voltage source inverters feeding power to the six-phase asymmetrical induction motor. Conventionally, the control algorithm helps to generate switching signals for IGBTs of VSIs using the vertices of the twelve-sided polygon, which yields harmonics (6k±1, k = 1, 3, 5...) in the pole voltage. Although, these harmonics are suppressed in the air gap MMF because of stator windings configuration (300 spatially shifted two groups of three-phase stator windings). However, it causes large harmonics currents to circulate in the stator, which is limited only by the stator circuit parameter. In this paper, the SVPWM control algorithm comprises two large active vectors and two neighboring medium active space vectors used to calculate dwell time and applied symmetrically to make only one transition during every sampling period. Hence, make it possible to maintain zero average value of 5th and 7th harmonics in the pole voltage. The control algorithm is implemented through MATLAB simulation and practically implemented using a digital signal controller. The effectiveness of the scheme is highlighted in results obtained from the prototype test setup.

Keywords: *Six-phase asymmetrical induction moto; harmonics components; Space Vector Pulse Width Modulation (SVPWM) and Voltage Source Inverter (VSI); microcontroller.*

1. INTRODUCTION

The multi-phase machine, in particular, a six-phase induction machine with two sets of the three-phase stator winding, spatially shifted by an electrical angle of 30° are referred to as the asymmetrical six-phase induction machine, has gained the attention of many researchers during the last three decades [1-3]. The specific attributes of this configuration include removal of the sixth harmonic torque pulsation and all space harmonics below the 11^{th} harmonics [4, 5]. Other benefits include improved noise characteristics, reduced stator copper loss, higher torque per ampere, and higher reliability at the system level [2].

With the advancement in control of power electronic converters, several modulation techniques have been introduced for multi-phase machines. These modulation schemes are mainly based on the space vector-based PWM method, while carrier-based PWM methods have been studied to a lesser extent. As per the theory of symmetrical components, switching vectors of asymmetrical six-phase can be symbolized as n-dimensional space with multiple two-dimensional sub-spaces (d-q), (x-y), and (0_1-0_2). The variable components which are mapped into the (d-q) subspace are related to actual energy conversion, while those of the non-electromechanical energy conversion is restricted in (x-y) and (0_1-0_2) subspaces. These components get suppressed in the air gap because of decoupling between stator and rotor. The large circulating harmonic currents in the stator are observed due to the small impedance associated with this subspace [6-9].

Various techniques have been reported in the literature to subdue the contents of these harmonic currents. One approach is to connect passive harmonics filters to reduce the level of harmonics pollution in the stator windings [10]. The second approach is on the machine side by modifying its assembly and/or stator winding [11]. The third approach on the supply side, by faithful PWM control strategies [6-9, 12-16], or switched capacitor filter for open-end windings [17]. This paper aims to explore the space vector-based approach to synthesize voltages of maximum amplitude in d-q plane and minimum in x-y plane, which are liable for large circulating harmonic currents. Therefore, it is essential to select a minimum of four active voltage vectors on d-q plane to make this possible and at the same time to gain control on x-y plane. The (01−02) plane is not in consideration because the two three-phase windings are star-connected with isolated neutrals [9].

The innovative approach of realizing symmetrical SVPWM is to exploit twelve large vectors of the largest polygon in the d-q plane [6], [8, 18, 19]. In this approach, two active space vectors adjacent to a reference vector and two null vectors are calculated in one switching period to realize the input reference voltage. Due to the similar approach of space vector modulation of three-phase voltage source converter, it leads to the generation of low order harmonics in VSI output voltage. The alternate way is to utilize four active vectors along with null vectors to control both the plane was introduced in [20]. The concept of discontinuous SVPWM [6], synchronized SVPWM [21], SVPWM operation with common-mode voltage reduction[16], SVPWM using 5 active vectors [22], and SVPWM based on 24-sector [7-9, 13] for six-phase IM were implemented. These modulation techniques result in numerous switching sequences or switching vectors. In the aspect of carrier-based PWM techniques, double zero sequence injection, analysis of SPWM, and zero-sequence injection along with SVPWM are carried out [14, 23].

Vector modulated six-phase system becomes complicated and requires more computational time. The switching pattern in these techniques described above produces asymmetrical waveforms in which more than two transitions (from low to high or vice-versa) occur on the corresponding PWM outputs

Volume 10, Issue 6
December 2021

ITEE Journal
Information Technology & Electrical Engineering

ISSN: - 2306-708X

in each sampling period. These results increase the switching frequency of the inverter and cause difficulties for the implementation of these strategies. Due to these reasons, the use of these vectors in the six-phase system is found to be rare.

This paper intends to develop a new algorithm based on two large and two medium vectors with some additional adaption for the realization of the space vector PWM techniques, which improves the accuracy, simplicity, and execution speed. Implementation of control algorithm on a modern digital signal controller and performance analysis carried out on a dual VSI inverter fed six-phase asymmetrical induction motor.

It is appropriate to use the vector delimiting the sector in which the reference voltage vector lies. Using large and medium vectors for removal of low order harmonics in space vector modulated six-phase system becomes complicated and requires more computational time. The switching pattern in these techniques described above produces asymmetrical waveforms. More than two transitions (from low to high or vice-versa) occur on the corresponding PWM outputs in each sampling period. These results increase the switching frequency of the inverter and cause difficulties for the implementation of these strategies. Due to these reasons, the use of these vectors in the six-phase system is found to be rare.

This paper intends to develop a new algorithm based on two large and two medium vectors with some additional adaption for the realization of the space vector PWM techniques, which improves the accuracy, simplicity, and execution speed. Implementation of control algorithm on a modern digital signal controller and performance analysis carried out on a dual VSI inverter fed six-phase asymmetrical induction motor.

Section 2 describes the SVPWM technique for a six-phase asymmetrical induction motor. Section 3 presents the SVPWM control algorithm. In Section 4, details of the experiment setup and the results of our experimental evaluation are discussed. The research work is concluded in Section 6.

2. SVPWM TECHNIQUE FOR SIX-PHASE ASYMMETRICAL INDUCTION MOTOR

The power circuit of the dual inverter comprises two three-leg VSI inverters (Inverter-1, Inverter-2). It consists of twelve self-commuting active switches (S_1-S_6 and S'_1-S'_6) with antiparallel freewheeling diode shown in Fig.1a. Typical space vectors for the two-level three-phase inverter as shown in Fig.1b, where the six active vectors constitute a regular hexagon with six equal sectors (1 to 6). As two distinct vectors of inverter-1 and inverter-2 with magnitude V_{dc} and phase displacement by $\pi/6$ radian are integrated, the corresponding resultant large active space vector of magnitude is obtained as shown in Fig.1c. Thus, the six-phase inverter comprises two three-phase inverters, 64 switching vectors demonstrated in Fig.2a, 12 Sectors, and the boundary of the voltage space phasor is a 12-sided polygon as shown Fig.1c.

To simplify the analysis, the switching state vector of the dual inverter is denoted by vectors in a six-dimensional vector space. These vectors can be transformed into three mutually orthogonal subspaces (d-q, x-y, 0_1-0_2) as given in equation (1)[9].

$$\begin{bmatrix} V_d \\ V_q \\ V_x \\ V_y \\ O+ \\ O- \end{bmatrix} = \frac{2}{6} * \begin{bmatrix} 1 & \cos\frac{2\pi}{3} & \cos\frac{4\pi}{3} & \cos\frac{\pi}{6} & \cos\frac{5\pi}{6} & \cos\frac{9\pi}{6} \\ 0 & \sin\frac{2\pi}{3} & \sin\frac{4\pi}{3} & \sin\frac{\pi}{6} & \sin\frac{5\pi}{6} & \sin\frac{9\pi}{6} \\ 1 & \cos\frac{4\pi}{3} & \cos\frac{8\pi}{3} & \cos\frac{5\pi}{6} & \cos\frac{\pi}{6} & \cos\frac{9\pi}{6} \\ 0 & \sin\frac{4\pi}{3} & \sin\frac{8\pi}{3} & \sin\frac{5\pi}{6} & \sin\frac{\pi}{6} & \sin\frac{9\pi}{6} \\ 1 & 1 & 1 & 0 & 0 & 0 \\ 0 & 0 & 0 & 1 & 1 & 1 \end{bmatrix} \begin{bmatrix} V_a \\ V_b \\ V_c \\ V_d \\ V_e \\ V_f \end{bmatrix} . \quad (1)$$

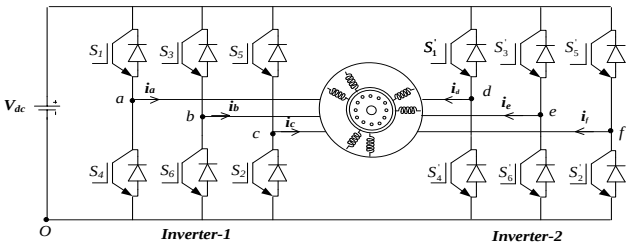

(a)

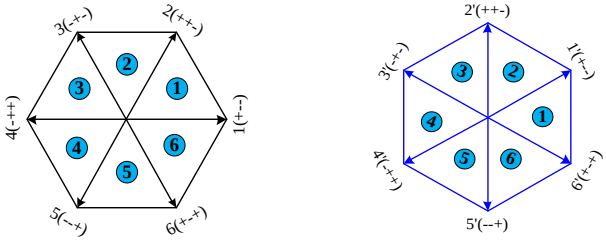

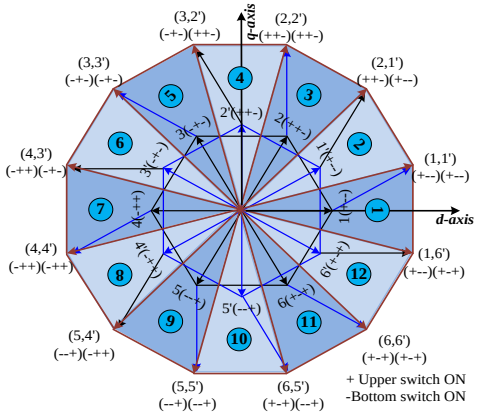

(b)

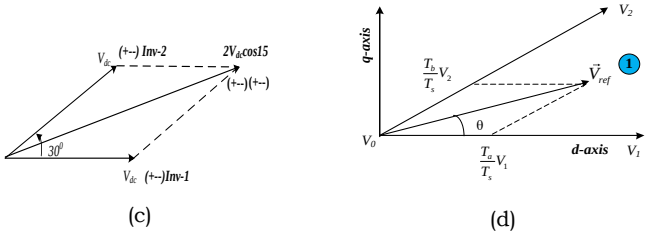

(c) (d)

Fig.1 Six-phase asymmetrical induction motor: (a) power circuit; (b) large space vectors formation; (c) resultant large space vector; and (d) sampled reference vector in a Sector-1

Initially, the SVPWM technique was synthesized in the d-q plane as shown in Fig.1b to generate the output voltages by

Volume 10, Issue 6
December 2021

ITEE Journal
Information Technology & Electrical Engineering

ISSN: - 2306-708X

utilizing only the outer larger active vectors to generate output voltages, based on the reference space vector. For the large vectors of the dual inverter, the generated voltage in the d-q plane can be expressed as

$$\vec{V}_K = \frac{2}{6}\left(2V_{dc}\cos 15^o\right)e^{j(K-1)\frac{\pi}{6}} \quad (2)$$

Where, switching sector, K=1, 2, 3….12. Let the reference vector V_{ref} falls in sector-1 and makes an angle, θ, concerning V1, as shown in Fig.1d. It can be realized with two adjacent active vectors (V_1, V_2) and one zero vector (V_0). The reference vector, V_{ref} synthesized by switching between V_1 and V_2 states for dwell time T_a and T_b, respectively, along the d-axis and q-axis as illustrated in Fig.1d. The value of dwell time can be calculated using the following equations,

$$T_a = 6\frac{V_{ref}}{(2V_{dc}\cos 15)}T_s \sin(\frac{\pi}{6}-\theta) \quad (3)$$

$$T_b = 6\frac{V_{ref}}{(2V_{dc}\cos 15)}T_s \sin\theta \quad (4)$$

Note that the above equations are derived assuming the reference vector V_{ref} falls in Sector-1. The dwell time in other sectors can also be provided with multiple of π/6 is subtracted from the actual angular displacement as given in equation (5).

$$\theta = \theta - (K-1)\frac{\pi}{6} \quad (5)$$

Modulation index (ma) is to be considered as unity for maximum utilization of dc bus. As ma varies from zero to one, the corresponding output voltage varies from zero to maximum utilization of dc link voltage in linear range. The equations (3) and (4) can be expressed as function of modulation index, ma, as follows:

$$T_a = 1.931 m_a T_s \sin(30-\theta) \quad (6)$$

$$T_b = 1.931 m_a T_s \sin(\theta) \quad (7)$$

Where,

$$m_a = \frac{\vec{V}_{ref}}{\frac{2}{6}\left(2V_{dc}\cos 15\right)\cos 15^o} \quad (8)$$

The maximum amplitude of the reference vector, $V_{ref(\max)}$, coincides with the radius of the largest circle that can be inscribed within the polygon shown in Fig.2a i.e., $V_{ref(max)}$=0.622Vdc. The maximum line-to-line fundamental RMS output voltage is $V_{(maxSVPWM)}$ = 0.7617 V_{dc}. Interestingly, the maximum fundamental phase voltage generated by 3-phase SVPWM using hexagonal structure is 0.577 V_{dc}; however, in the case of 6-phase polygonal structure, it is 0.622 V_{dc}.

$$\frac{V_{\max}(SVPWM)_{6-phase}}{V_{\max}(SVPWM)_{3-phase}} = \frac{0.622}{0.577} = 1.07 \quad (9)$$

Thus, in SVPWM controlled dual inverter, an increase of 7% in output voltage is obtained due to the presence of 6k±1 harmonics in the average pole waveforms[19].

The dual inverter is operated in both complex planes, d-q and x-y, to suppress these harmonics 5th and 7th in pole voltages,. To achieve the above reference signal, Vref should produce the fundamental component in the d−q plane and simultaneously maintain the zero average value of harmonic components in x-y plane [6]. Therefore, using four active vectors (two large and two medium space vectors) into each switching period helps in maintaining zero average value in the x-y plane [7-9].

Calculation of four dwell times labeled as Tal, Tam, Tbl, Tbm is required for the use of four active space vectors per switching period. As both medium and large space vectors lie on the identical lines as shown in Fig.3a, the equation (6) and (7) for Ta and Tb calculations are still valid, provided calculated times Ta and Tb must be suitably distributed among large and medium space vectors as given in equation (10).

$$T_a = T_{al} + T_{am}\ ,\ T_b = T_{bl} + T_{bm}. \quad (10)$$

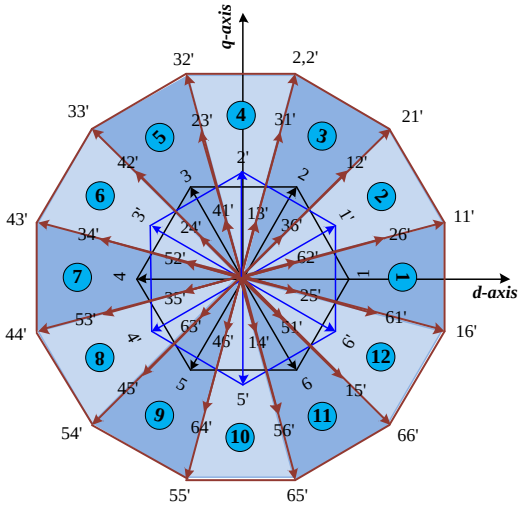

(a)

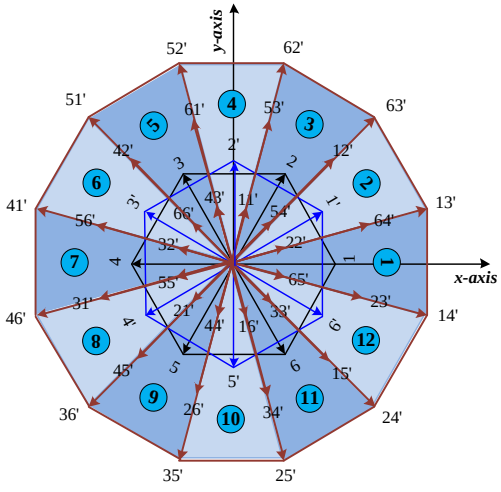

(b)

Fig.2: Space vector of a dual inverter VSI (a) d-q plane (b) x-y plane

The position of active space vectors (11' and 26') in the x-y plane (Fig. 3a) helps to obtain zero average voltage, as per the following constraints:

$$T_{al}\,|\overline{V_s}| = T_{am}\,|\overline{V_m}| \quad (11)$$

$$T_{bl}\,|\overline{V_s}| = T_{bm}\,|\overline{V_m}| \quad (12)$$

Volume 10, Issue 6
December 2021

ITEE Journal
Information Technology & Electrical Engineering

ISSN: - 2306-708X

By solving the equation (10)-(12), the dwell times for active space vectors are evaluated as

$$T_{al} = \frac{|\overline{V_m}|}{|\overline{V_m}|+|\overline{V_s}|} T_a \quad , \quad T_{bl} = \frac{|\overline{V_m}|}{|\overline{V_m}|+|\overline{V_s}|} T_b \qquad (13)$$

$$T_{am} = \frac{|\overline{V_s}|}{|\overline{V_m}|+|\overline{V_s}|} T_a \quad , \quad T_{bm} = \frac{|\overline{V_s}|}{|\overline{V_m}|+|\overline{V_s}|} T_b \qquad (14)$$

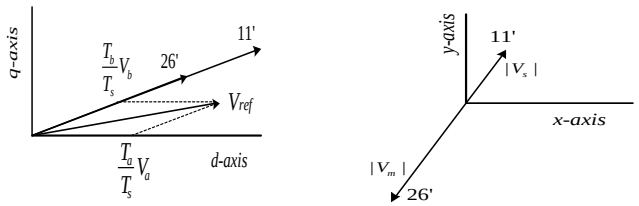

(a)

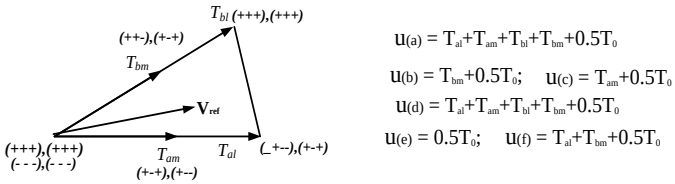

$u_{(a)} = T_{al}+T_{am}+T_{bl}+T_{bm}+0.5T_0$

$u_{(b)} = T_{bm}+0.5T_0$; $u_{(c)} = T_{am}+0.5T_0$

$u_{(d)} = T_{al}+T_{am}+T_{bl}+T_{bm}+0.5T_0$

$u_{(e)} = 0.5T_0$; $u_{(f)} = T_{al}+T_{bm}+0.5T_0$

(b)

Fig. 3: Calculation of dwell times: (a) generalized method for active vectors calculation; and (b) active vector and dwell time in in sector 1.

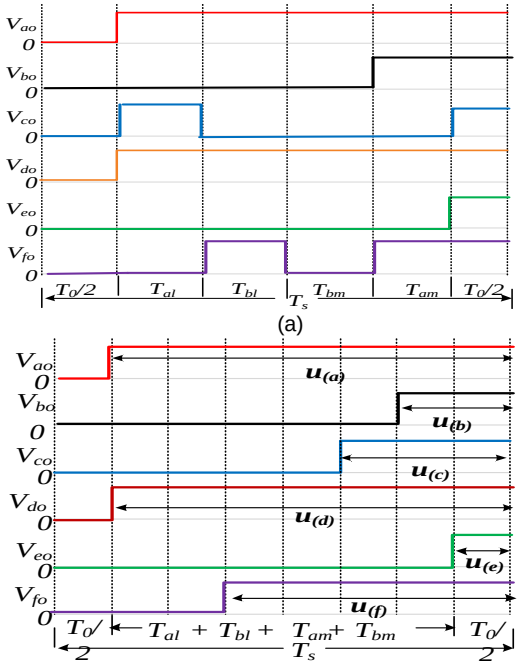

Fig. 4: Switching sequence: (a) conventional; and (b) modified switching sequence for θ<15°.

The magnitudes of large (V_l), medium (V_m), and small (V_s) space vectors are 1.931 V_{dc}, 1.414 V_{dc}, and 0.5176 V_{dc}, respectively. The numerical values for dwell factors depict that 73.2% of the application time of active space vectors is applied to large space vectors, while 26.7% of the time is applied to medium space vectors. Applying the principle of volt-second for SVPWM based on large and medium space vectors indicates that for any given reference space vector magnitude, the corresponding fundamental at the output is reduced to 92.5%. Thus, the amplitude of the reference space vector is pre-multiplied by the factor 1.08 to maintain the modulator gain equal to unity in the linear region.

Switching pattern in a twelve-sided polygon using four active vectors offers asymmetrical pole waveforms and lead to discontinuity in PWM pole voltage waveforms, as shown in Fig. 3c. In other words, switching ON/OFF, which appeared more than once, and half-wave symmetry during one sampling period vanishes. As a consequence number of switching is increased and does not meet the design requirements.

Instead of forcing vectors to travel along the large and medium vectors sequentially, the calculated dwell time interval using equations (13)-(14) is applied symmetrically to achieve only one transition during every sampling period. Note that these vectors are used only to calculate dwell time u(i), where i= a,b,c,d,e,f as shown in Fig. 3b. The switch with the largest dwell time is applied first and regressively applied to other switches, as shown in Fig.3d. Using this, various calculations for voltage vectors applying time and its selection according to the sector number described are eliminated. The selection of applied vectors is independently controlled. It relies on the position of a reference vector in a sector-1 as summarized in Table I. Observing the resultant switching sequence for θ<15°, shows identical sequence obtained while for θ>15° sequence slightly differs. Consequently, reduction of 5th and 7th can be accomplished without subdividing sector for calculation though obtain results are finally placed in 24 sectors (i.e., θ<15° and θ>15°).

The proposed switching pattern yields reduction in the switching frequency of the inverters and permits ease of implementation. The dwell times of all the top six switches for corresponding sectors are presented in Table II. The maximum magnitude of the reference vector using the proposed control algorithm has a magnitude of 0.577 V_{dc} equal to the reference vector value gained with continuous carrier-based methods that utilize injection of third harmonic signals.

Table 1: Calculation of dwell times in all the sector

Sector	ON- Time Sector
1	u(a)= $T_{al}+T_{am}+T_{bl}+T_{bm}+(T_0/2)$; u(b)=$T_{bm}$+ ($T_0$/2); u(c)= $T_{am}+(T_0/2)$; u(d)= $T_{al}+T_{am}+T_{bl}+T_{bm}+(T_0/2)$; u(e)= ($T_0$/2); u(f)=$T_{al}+T_{bm}$+ ($T_0$/2);
2	u(a)= $T_{al}+T_{am}+T_{bl}+T_{bm}+(T_0/2)$; u(b)= $T_{am}+T_{bl}+(T_0/2)$; u(c)= (T_0/2); u(d)= $T_{al}+T_{am}+T_{bl}+T_{bm}+(T_0/2)$; u(e)= $T_{bm}+(T_0/2)$; u(f)= $T_{am}+(T_0/2)$;
3	u(a)= $T_{al}+T_{am}+T_{bl}+(T_0/2)$; u(b)= $T_{al}+T_{bl}+T_{bm}+(T_0/2)$; u(c)= ($T_0$/2); u(d)= $T_{al}+T_{am}+T_{bl}+T_{bm}+(T_0/2)$; u(e)= $T_{am}+T_{bl}+(T_0/2)$; u(f)= (T_0/2);
4.	u(a)= $T_{al}+T_{bm}+(T_0/2)$; u(b)= $T_{al}+T_{am}+T_{bl}+T_{bm}+(T_0/2)$; u(c)= ($T_0$/2); u(d)= $T_{al}+T_{am}+T_{bl}+(T_0/2)$; u(e)= $T_{al}+T_{bl}+T_{bm}+(T_0/2)$; u(f)= ($T_0$/2);
5	u(a)= $T_{am}+(T_0/2)$; u(b)= $T_{al}+T_{am}+T_{bl}+T_{bm}+(T_0/2)$; u(c)= $T_{bm}+(T_0/2)$; u(d)= $T_{al}+T_{bm}+(T_0/2)$; u(e)= $T_{al}+T_{am}+T_{bl}+T_{bm}+(T_0/2)$; u(f)= ($T_0$/2);
6	u(a)= (T_0/2); u(b)= $T_{al}+T_{am}+T_{bl}+T_{bm}+(T_0/2)$; u(c)= $T_{am}+T_{bl}+(T_0/2)$; u(d)= $T_{am}+(T_0/2)$; u(e)= $T_{al}+T_{am}+T_{bl}+T_{bm}+(T_0/2)$; u(f)= $T_{bm}+(T_0/2)$;
7	u(a)= (T_0/2); u(b)= $T_{al}+T_{am}+T_{bl}+(T_0/2)$; u(c)= $T_{al}+T_{bl}+T_{bm}+(T_0/2)$; u(d)= ($T_0$/2); u(e)= $T_{al}+T_{am}+T_{bl}+T_{bm}+(T_0/2)$; u(f)= $T_{bl}+T_{bm}+(T_0/2)$;
8	u(a)= (T_0/2); u(b)= $T_{al}+T_{bm}+(T_0/2)$; u(c)= $T_{al}+T_{am}+T_{bl}+T_{bm}+(T_0/2)$; u(d)= ($T_0$/2); u(e)= $T_{al}+T_{am}+T_{bl}+(T_0/2)$; u(f)= $T_{al}+T_{bl}+T_{bm}+(T_0/2)$;
9	u(a)= $T_{bm}+(T_0/2)$; u(b)= $T_{am}+(T_0/2)$; u(c)= $T_{al}+T_{am}+T_{bl}+T_{bm}+(T_0/2)$; u(d)= ($T_0$/2); u(e)= $T_{al}+T_{bm}+(T_0/2)$; u(f)= $T_{al}+T_{am}+T_{bl}+T_{bm}+(T_0/2)$;
10	u(a)= $T_{bl}+T_{am}+(T_0/2)$; u(b)= (T_0/2); u(c)=$T_{al}+T_{am}+T_{bl}+T_{bm}+(T_0/2)$;

Volume 10, Issue 6
December 2021

ITEE Journal
Information Technology & Electrical Engineering

ISSN: - 2306-708X

	u(d)=T_{bm}+(T_0/2); u(e)=T_{am}+(T_0/2); u(f)= T_{al}+T_{am}+T_{bl}+T_{bm}+(T_0/2);
11	u(a)= T_{al}+T_{bl}+T_{bm}+(T_0/2); u(b)= (T_0/2); u(c)= T_{al}+T_{am}+T_{bl}+(T_0/2); u(d)= T_{am}+T_{bl}+(T_0/2); u(e)= (T_0/2); u(f)= T_{al}+T_{am}+T_{bl}+T_{bm}+(T_0/2);
12	u(a)= T_{al}+T_{am}+T_{bl}+T_{bm}+(T_0/2); u(b)= (T_0/2); u(c)= T_{al}+T_{bm}+(T_0/2); u(d)= T_{al}+T_{bl}+T_{bm}+(T_0/2); u(e)= (T_0/2); u(f)= T_{al}+T_{am}+T_{bl}+(T_0/2);

3. IMPLEMENTATION OF SVPWM CONTROL ALGORITHM

A Digital Signal Controller (STM32F4 ARM-Cortex M4) is used to implement control algorithms that utilize high-speed counters/timers with capture compare registers (CCR) to generate switching signals IGBTs of the dual inverter. The following steps are involved for the implementation of SVPWM techniques:

1. Calculation of V_{ref}*; and angle θ
2. Sector Identification
3. Calculation of dwell Time
4. Generation of Modulation Signals V_a*, V_b*, V_c*, V_d*, V_e*, V_f*.

To implement the control algorithm, the timer is utilized to generate an interrupt at every sample time Ts for calculation of Vref and angle θ. Advance timers (Timer1 & Timer 8) with capture compare registers are utilized to calculate dwell time and fed to capture compare register accordingly. ON time for each switch is calculated at every sampling interval. Meanwhile, the hardware PWM unit keeps working in the background, transforming the modulation signals from the previous calculation to appropriate pulses for the gate driver circuits. As machine's control algorithms are complicated, the PWM modulator shouldn't burden the controller.

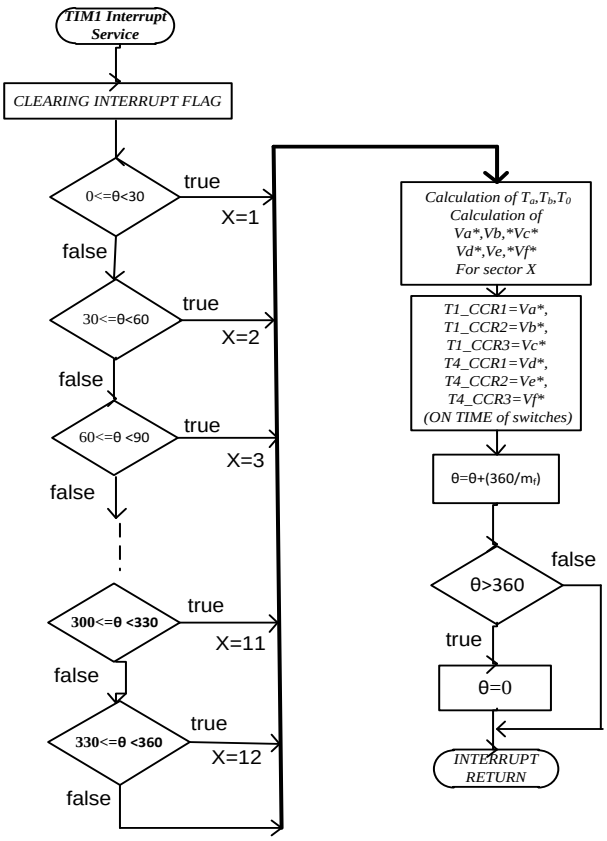

Fig. 5 Flowchart for SVPWM algorithm and PWM generation

Thus, it should be simple, fast and should occupy less memory space. The space vector PWM modulator algorithm is simple and requires few mathematical calculations to provide modulation signals. Fig. 4 shows the flowchart of interrupt service routine responsible for generating PWM modulator and generated PWM pulses using capture compare register.

4. RESULTS AND DISCUSSIONS

The Simulink model of the six-phase induction motor is developed to implement SVPWM algorithms and simulation studies. A prototype test setup of a six-phase, star-connected asymmetrical induction motor with 1.5kW, 200 V, 50 Hz, 4-pole has been developed to verify the accuracy and performance of the control scheme presented. The prototype test setup consists of SEMIKRON make dual VSI inverter modules supplied by gate pulses generated by the STM32F407 controller, as shown in Fig. 6. Two units voltage source inverters operate with the specification of Vdc=180V, f = 50 Hz, ma =1.0, and 3kHz switching frequency.

Volume 10, Issue 6
December 2021

ITEE Journal
Information Technology & Electrical Engineering

ISSN: - 2306-708X

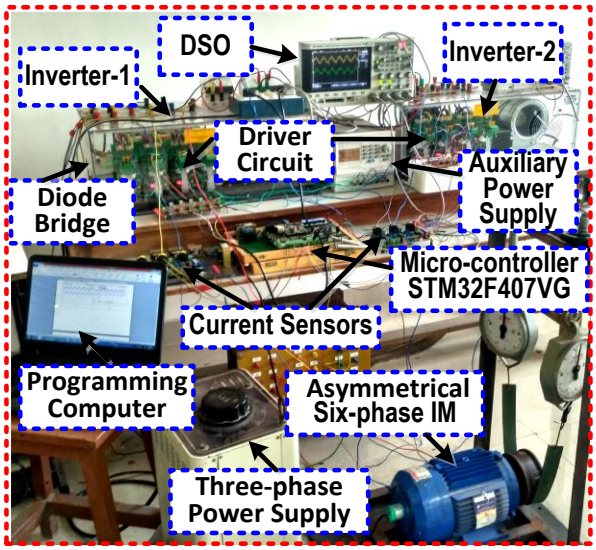

Fig. 6: Experimental test bench of six-phase asymmetrical induction motor

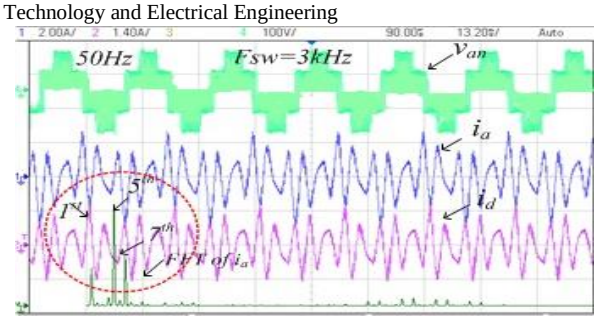

(c)

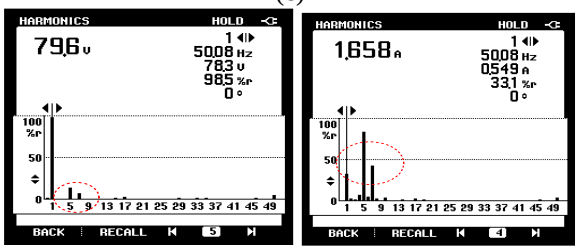

(d)

Fig.7: Experimental results: (a) reference wave, carrier wave, switching signal, and harmonic spectra of pole voltage; (b) phase voltages (v_{an},v_{dn}) and FFT of phase voltages; (c) phase voltage, stator currents (i_a ,i_d) and its harmonic spectra at 50Hz output frequencies; and (d) FFT of phase-voltage and line current.

A. SVPWM using Two Large Active Vectors

Fig. 7 shows the experimental waveforms of phase voltage (van), stator currents (i_a , i_d) of six-phase asymmetric induction motor and harmonic spectra of stator currents (i_a) and phase voltage (v_{an}), at distinct inverter output frequency 50Hz. Fig. 7a shows the modulated reference and carrier wave recorded using DAC of the controller. As expected the presence of 6k±1 harmonics in pole voltage which is observed in Fig.7a result into a large 5th and 7th stator harmonics current as shown in Fig. 7c. These harmonics components appear more dominantly in stator current as shown in Fig.7c-d, and controlled by stator impedance only. The harmonic spectra of phase-voltage and line current are also recorded through fluke power quality analyzer and presented in Fig.7e-f.

B. SVPWM using Proposed Control Algorithm

Fig. 8 shows the experimental waveforms of phase voltages (v_{an},v_{dn}), and stator currents (i_a , i_d) and its FFT spectra for two distinct inverter output frequencies 30Hz and 50Hz with proposed control algorithm fed six-phase asymmetrical induction motor. Fig. 8a shows the modulated reference and carrier wave recorded using DAC of controller. The stator currents (i_a, i_d) drawn by motor and phase voltage(v_{an}) at terminal of six-phase induction motor with different inverter output frequencies are shown in Fig. 8c and Fig. 8d.

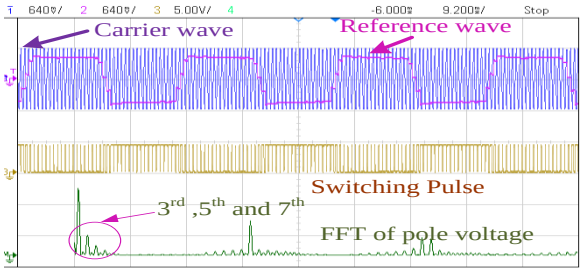

(a)

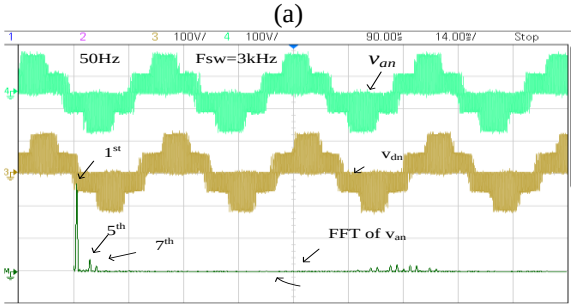

(b)

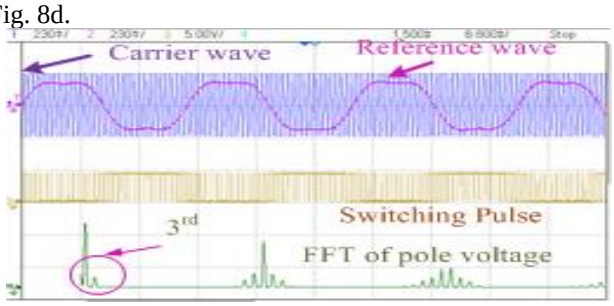

(a)

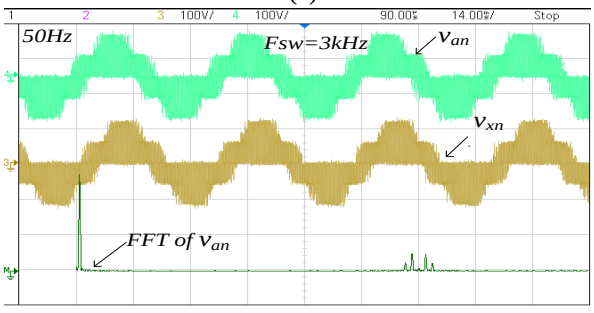

(b)

Volume 10, Issue 6
December 2021

ITEE Journal
Information Technology & Electrical Engineering

ISSN: - 2306-708X

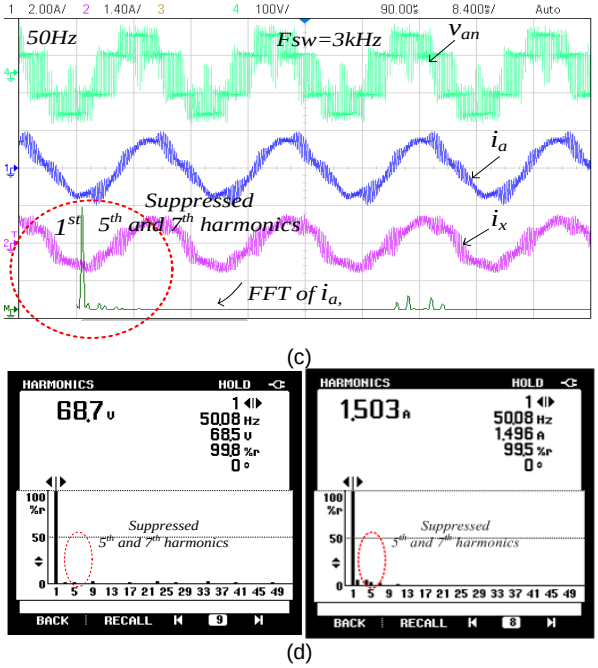

Fig. 8: Experimental results of proposed control algorithm: (a) reference wave, carrier wave, switching signal, and harmonic spectra of pole voltage; (b) phase voltages (v_{an},v_{dn}) and FFT of phase voltages; (c) phase voltage(v_{an}), stator currents (i_a ,i_d) and its harmonic spectra at 50Hz output frequency; (d), and (e) FFT of phase-voltage and line current.

It is observed in the figure that significant reduction in stator current harmonics due to the absence of 6k±1 harmonics in-phase voltage as shown in Fig. 8b. This experimental result reveals that by employing the proposed control algorithm, there is a significant reduction in the stator harmonic current and complexity of hardware implementation.

5. CONCLUSIONS

In this paper, SVPWM control techniques using a large active vector for a six-phase asymmetrical induction motor have been implemented and analyzed. The results show higher stator harmonic current, particularly dominant 5th and 7th harmonics, than fundamental stator current. It leads to higher stator loss. Therefore, a new control algorithm based on dwell time calculation and symmetrically controlled switching sequence are proposed to eliminate the harmonics mentioned above. This scheme uses four active vectors for the calculation of dwell time, and the selection of the applied vector is independently controlled and relies on the position of a reference vector in a sector. This technique offers features such as ease of implementation, cost-effectiveness, and reduced computational burden. The effectiveness of the proposed scheme is excellent for suppressing the 5th, and 7th harmonics, which is verified in both simulation and experimental studies.

REFERENCES

[1] E. Levi, R. Bojoi, F. Profumo, H. Toliyat, and S. Williamson, "Multiphase induction motor drives-a technology status review," *IET Electric Power Applications*, vol. 1, no. 4, pp. 489-516, July 2007.

[2] E. Levi, F. Barrero, and M. J. Duran, "Multiphase machines and drives-Revisited," *IEEE Transactions on Industrial Electronics*, vol. 63, no. 1, pp. 429-432, Jan. 2016.

[3] M. J. Duran and F. Barrero, "Recent advances in the design, modeling, and control of multiphase machines—Part II," *IEEE Transactions on Industrial Electronics*, vol. 63, no. 1, pp. 459-468, Jan. 2016.

[4] E. A. Klingshirn, "High phase order induction motors-Part I-Description and theoretical considerations," *IEEE Transactions on power Apparatus and Systems*, vol. PAS-102, no. 1, pp. 47-53, Jan. 1983.

[5] R. Nelson and P. Krause, "Induction machine analysis for arbitrary displacement between multiple winding sets," *IEEE Transactions on power Apparatus and Systems*, no. 3, pp. 841-848, 1974.

[6] D. Hadiouche, L. Baghli, and A. Rezzoug, "Space-vector PWM techniques for dual three-phase AC machine: analysis, performance evaluation, and DSP implementation," *IEEE Transactions on Industry Applications*, vol. 42, no. 4, pp. 1112-1122, 2006.

[7] R. Maurya and M. S. Shaikh, "Simplified implementation of SVPWM techniques for a Six-phase machine with reduced current distortion features," *IET Electric Power Applications*, pp. 1-1, 2019.

[8] K. Marouani, L. Baghli, D. Hadiouche, A. Kheloui, and A. Rezzoug, "A new PWM strategy based on a 24-sector vector space decomposition for a six-phase VSI-fed dual stator induction motor," *IEEE Transactions on Industrial Electronics*, vol. 55, no. 5, pp. 1910-1920, 2008.

[9] M. S. Shaikh and R. Maurya, "Realization of 24-Sector SVPWM with New Switching Pattern for Six-Phase Induction Motor Drive," *IEEE Transactions on Power Electronics*, vol. 34, no. 6, pp. 5079-5092, 2018.

[10] E. A. Klingshirn, "Harmonic filters for six-phase and other multiphase motors on voltage source inverters," *IEEE Transactions on Industry Applications*, vol. IA-21, no. 3, pp. 588-594, 1985.

[11] D. Hadiouche, H. Razik, and A. Rezzoug, "On the modeling and design of dual-stator windings to minimize circulating harmonic currents for VSI fed AC machines," *IEEE Transactions on Industry Applications*, vol. 40, no. 2, pp. 506-515, 2004.

[12] K. Marouani, L. Baghli, D. Hadiouche, A. Kheloui, and A. Rezzoug, "Discontinuous SVPWM techniques for double star induction motor drive control," in *IECON 2006-32nd Annual Conference on IEEE Industrial Electronics*, Paris, 2006, pp. 902-907.

[13] P. R. Rakesh and G. Narayanan, "Analysis of sine-triangle and zero-sequence injection modulation schemes for split-phase induction motor drive," *IET Power Electronics*, vol. 9, no. 2, pp. 344-355, 2016.

[14] P. Rakesh and G. Narayanan, "Investigation on Zero-Sequence Signal Injection for Improved Harmonic Performance in Split-Phase Induction Motor Drives," *IEEE Transactions on Industrial Electronics*, vol. 64, no. 4, pp. 2732-2741, April 2016.

[15] K. Chinmaya and G. K. Singh, "Experimental analysis of various space vector pulse width modulation (SVPWM) techniques for dual three-phase induction motor drive," *International Transactions on Electrical Energy Systems*, vol. 29, no. 1, pp. e2678, 2019.

[16] J. Zheng, F. Rong, P. Li, S. Huan, and Y. He, "Six-phase SVPWM with common-mode voltage suppression," *IET Power Electronics*, vol. 11, no. 15, pp. 2461-2469, 2018.

[17] N. A. Azeez, K. Gopakumar, J. Mathew, and C. Cecati, "A harmonic suppression scheme for open-end winding split-phase IM drive using capacitive filters for the full speed range," *IEEE Transactions on Industrial Electronics*, vol. 61, no. 10, pp. 5213-5221, 2014.

[18] M. S. A. Shaikh and R. Maurya, "A Comparative Study of PWM Techniques for Multiphase Induction Motor Drives," *International Journal of Emerging Electric Power Systems*, vol. 19, no. 5, 2018.

[19] K. Gopakumar, V. Ranganathan, and S. Bhat, "An efficient PWM technique for split phase induction motor operation using dual voltage source inverters," in *Industry Applications Society Annual Meeting, 1993., Conference Record of the 1993 IEEE*, Toronto, Ontario, Canada., 1993, pp. 582-587.

[20] Y. Zhao and T. A. Lipo, "Space vector PWM control of dual three-phase induction machine using vector space decomposition," *IEEE Transactions on Industry Applications*, vol. 31, no. 5, pp. 1100-1109, Sep. 1995.

[21] C. Wang, K. Wang, and X. You, "Research on Synchronized SVPWM Strategies Under Low Switching Frequency for Six-Phase VSI-Fed Asymmetrical Dual Stator Induction Machine," *IEEE Transactions on Industrial Electronics*, vol. 63, no. 11, pp. 6767-6776, 2016.

[22] W. Kun, Y. Xiaojie, W. Chenchen, sand Z. Minglei, "An equivalent dual three-phase SVPWM realization of the modified 24-sector SVPWM strategy for asymmetrical dual stator induction machine," in *2016 IEEE Energy Conversion Congress and Exposition (ECCE)*, Milwaukee, WI, 2016, pp. 1-7.

[23] J. Prieto, E. Levi, F. Barrero, and S. Toral, "Output current ripple analysis for asymmetrical six-phase drives using double zero-sequence injection PWM," in *IECON 2011-37th Annual Conference on IEEE Industrial Electronics Society*, Australia, 2011, pp. 3692-3697.

AUTHOR PROFILES

Shaikh Mo. Suhel A received the B.E. degree in electrical engineering from Veer Narmad South Gujarat University, Surat, India, in 2006, and the M.Tech. degree with specialization in industrial electronics and the Ph.D. degree in electrical engineering from the Sardar Vallabhbhai National Institute of Technology, Surat, India, in 2010 and 2020, respectively. He is currently an Assistant Professor with the Department of Electrical Engineering, R.N.G.Patel Institute of Technology Bardoli, Surat, India. His research interests include multiphase induction motor and power electronics converter for drives application, high power factor based dc-dc converter, and multilevel inverter.

Vamja Rajan Vinodray received a B.E. Degree in electrical engineering from the Lalbhai Dalpatbhai College of Engineering, Ahmedabad, India, in 2013, the M.Tech. Degree from the Sardar Vallabhbhai National Institute of Technology, Surat, India, in 2016. Currently, he is looking forward to his Ph.D. degree from Sardar Vallabhbhai National Institute of Technology, Surat, India. His research interests include renewable energy systems, electrical drives, power quality.